Journal of Marine Research, 60, 583–604, 2002

Intermingling of two *Pseudocalanus* species on Georges Bank

by D. J. McGillicuddy, Jr.[1] and A. Bucklin[2]

ABSTRACT

Physical and biological controls on the springtime distributions of *Pseudocalanus moultoni* and *P. newmani* on Georges Bank are examined by assimilating observations into a coupled physical-biological model. Monthly snapshots of abundance are derived from U.S. GLOBEC Georges Bank broad-scale surveys during 1997. The forward problem is posed as an advection-diffusion-reaction equation for the copepod concentration. The adjoint method of data assimilation is used to invert for the biological sources and sinks implied by the observed changes in abundance between surveys and the flow during the intervening period. Based on this analysis, the two species appear to have distinct population centers in the late winter/early spring: *P. moultoni* on the northwest flank of the Bank and *P. newmani* on the Northeast Peak and the southern tip of Browns Bank. As the growing season progresses, the clockwise circulation around Georges Bank blends reproducing (but not interbreeding) animals from the two source regions, causing their distributions to overlap by early summer. The springtime evolution of *Pseudocalanus* distributions in this region is driven by a complex mixture of hydrodynamic transport and species-specific population dynamics, including both growth and mortality.

1. Introduction

Calanoid copepods of the genus *Pseudocalanus* are some of the most abundant (in terms of number per unit volume) mesozooplankton on Georges Bank and in the Gulf of Maine (Davis, 1987). Two sibling species, *P. moultoni* and *P. newmani,* occur sympatrically in the region (Frost, 1989). Their naupliar and copepodite stages are preferred prey items for larval cod and haddock spawned on Georges Bank, thus potentially linking variability in recruitment of commercially important fish stocks with fluctuations in the abundance of these copepods (Laurence, 1974; Cohen and Lough, 1982). Despite the importance of the species to the ecosystem dynamics of the region, their population dynamics have remained enigmatic for decades (cf. Corkett and McLaren, 1978; Frost, 1989; McLaren *et al.,* 1989; Bucklin *et al.,* 2001). Slight differences in morphology, meristics and morphometrics attest to their taxonomic distinction (Frost, 1989). However, the two species of the genus are so

1. Department of Applied Ocean Physics and Engineering, Woods Hole Oceanographic Institution, Woods Hole, Massachusetts, 02543, U.S.A. ***email: dmcgillicuddy@whoi.edu***

2. Ocean Process Analysis Laboratory, University of New Hampshire, Durham, New Hampshire, 03824, U.S.A.

similar morphologically that routine sorting of large numbers of individuals is not practical. Recent application of molecular genetic techniques has made it possible to identify individuals accurately and quantify the relative proportions of the two species in samples of *Pseudocalanus* (Bucklin *et al.,* 1998). Used together with the absolute abundance of the combined species, this approach has allowed the first detailed regional-scale maps quantifying the distributions of *P. moultoni* and *P. newmani* on Georges Bank (Bucklin *et al.,* 2001). These observations provide an opportunity to study the physical-biological interactions that control variations in the distribution and abundance of the two sibling species.

Various aspects of the oceanographic ecology of the combined species have been studied using coupled physical-biological models. Davis (1984a) examined the effects of circulation and population dynamics in producing spatial patterns in stage structure observed during a survey on Georges Bank in February 1975. In this model, adult females from the Gulf of Maine are transported onto the Bank along its northwestern flank. High phytoplankton concentrations on the Bank relieve them of food limitation, and they begin producing eggs. The eggs mature into naupliar and copepodite stages as they are advected by the clockwise flow around the Bank. Because the organisms' developmental period is comparable to the residence time of water on the Bank, a clear pattern is generated in the around-Bank stage distribution: one that is similar to that observed in Davis' February 1975 survey.

The processes controlling seasonal changes in the distribution of adult *Pseudocalanus* spp. in the Gulf of Maine/Georges Bank region were investigated by McGillicuddy *et al.* (1998), based on ten years of sampling (1977–1987) from the Marine Resources Monitoring, Assessment, and Prediction Program (MARMAP). Two population centers were clearly evident in that analysis: one on Georges Bank and one in the near-coastal waters of the western Gulf of Maine. Inversion of these data indicated that the two populations are relatively isolated on a time scale characteristic of the organisms' developmental period (two months), suggesting that each may be self-sustaining. However, use of the term "population" in the context of Davis (1984a) and McGillicuddy *et al.* (1998) is potentially problematic because both studies are based on data that do not distinguish the two species of *Pseudocalanus.*

New observations from the U.S. GLOBEC Georges Bank broad-scale sampling program facilitate species-specific studies of *P. moultoni* and *P. newmani.* Monthly surveys from February through June of 1997 provide a set of quantitative synoptic maps of adults of both *Pseudocalanus* species (Bucklin *et al.,* 2001). In this study, the monthly snapshots are assimilated into a coupled physical-biological model. The adjoint method is used to infer the biological sources and sinks required to match the observed organismal distributions given specified flow fields. Thus, the inverse model constitutes a framework for dynamical interpolation between surveys. The resulting solutions are used to elucidate the mechanisms regulating the concentration of *P. moultoni* and *P. newmani* on Georges Bank. By linking the monthly surveys together in

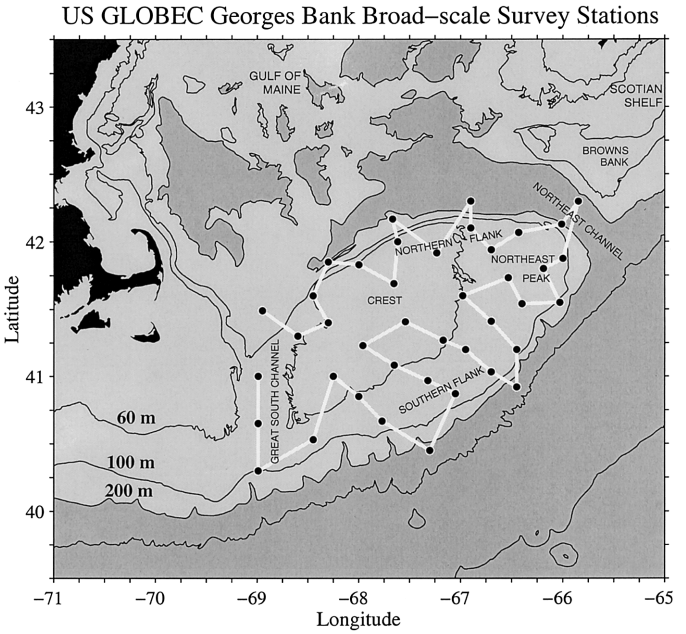

Figure 1. The U.S. GLOBEC Georges Bank Program broad-scale sampling station plan.

this manner, a conceptual model for the springtime evolution of the distribution and abundance of the two species is produced.

2. Methods

Abundance estimates for adult female *P. moultoni* and *P. newmani* were derived from the U.S. GLOBEC Georges Bank broad-scale surveys (Fig. 1) from February through June of 1997, as described in Bucklin *et al.* (2001). Samples were analyzed from two vertical strata: 0–15 m (surface) and 15–40 m (subsurface). Surface and subsurface abundance patterns of the two species were generally coherent, so the two strata were summed for this study to compute integrated abundance over the 0–40 m depth interval. These data were log-transformed and objectively analyzed onto a finite-element mesh. The logarithmic transformation was required in order to make the statistics of the data more normal, in accordance with the assumptions used in the objective analysis technique. The analyzed fields were then transformed back to abundance, from which the vertically-averaged concentration was computed by dividing by the water column depth.[3] The resulting

3. It has been noted that mapping log-transformed data with subsequent back-transformation can introduce a downward bias in the resulting mean field (e.g. Foote and Stefánsson, 1993; Romaine *et al.,* 2002). We estimated the magnitude of the bias by differencing the back-transformed results of the objective analysis with the original data at each station location. On average the bias was only 400 individuals m^{-2}. Therefore this effect represents a relatively minor source of error in the present application.

concentration fields were then fed into the inversion procedure. Details of each element of the methodology are summarized below.

a. Sample collection and genetic assays

Zooplankton samples were collected for molecular analysis at 18 standard stations during broad-scale surveys in March, April, and May; 10 stations were sampled in February and 17 in June 1997. Adult female *Pseudocalanus* spp. were selected randomly from alcohol-preserved sub-samples of each collection. Individual copepods were identified to species using a simple molecular protocol, competitive multiplexed species-specific PCR (SS-PCR), which discriminates between *P. moultoni* and *P. newmani* based on the DNA sequence of a selected gene, mitochondrial cytochrome oxidase I (see Bucklin *et al.,* 1999, 2001; Bucklin, 2000).

At least 20 female *Pseudocalanus* spp. in each sub-sample were identified to species by SS-PCR. Failed PCRs ranged from zero (usually) to 3 for a given sample; additional PCRs were done as necessary to meet the target size of 20 per sample. A total of 2935 *Pseudocalanus* spp. was assayed by SS-PCR from the February to June, 1997 broad-scale surveys (see Bucklin *et al.* (2001) for detailed information). The relative abundance of each species among the 20 individuals was used to estimate the abundance of each species by multiplying by the total number per square meter of female *Pseudocalanus* spp. in the sample, as determined by the U.S. GLOBEC Zooplankton Sorting Group at the University of Rhode Island (E. G. Durbin and P. Garrahan, University of Rhode Island, unpublished data; also see http://globec.whoi.edu).

b. Objective analysis

Construction of distributional maps suitable for input into models requires an algorithm by which irregularly spaced observations can be interpolated onto an arbitrary grid. Objective analysis is a technique that minimizes the expected error (in a least squares sense) at each analysis point via a linear combination of the neighboring observations. Each data point is weighted according to its space/time distance from the analysis point and a four-dimensional correlation function derived from an ensemble of prior data. Thus, statistical information about the measured field is used to optimize the resulting map. This procedure has been used routinely for nearly three decades in open-ocean applications where the underlying statistics are fairly homogeneous and well-behaved (Bretherton *et al.,* 1976; Freeland and Gould, 1976).

Objective analysis in coastal domains is a much more difficult problem for essentially two reasons. First, the presence of a coastline imposes geometrical constraints that are not easily handled analytically. Second, coastal processes are in general strongly impacted by topography, which results in highly non-uniform statistics. For example, Petrie and Dean-Moore (1996) demonstrated that correlation length scales of physical properties on the Scotian shelf were generally larger in the along-isobath direction than across isobaths. He *et al.* (1997) have implemented these aspects into an objective analysis procedure based

on the original algorithm developed by Bretherton *et al.* (1976). The basic idea is that a set of domain-wide correlation scales are modulated by the local bathymetric gradients, such that the anisotropy with respect to along- versus across-isobath correlations is explicit.

For the purposes of this study, *Pseudocalanus* distributions were mapped using the He *et al.* (1997) algorithm, using the same correlation scales that Lynch *et al.* (1996) used for objective analysis of hydrographic measurements. Sensitivity analysis showed that the resulting maps of *Pseudocalanus* distributions on Georges Bank were generally robust over a reasonable range of choices for the global correlation scales (20–60 km). However, rigorous assessment of the spatial and temporal covariance statistics of *Pseudocalanus,* as well as other zooplankton, is clearly needed in future research. Recent developments in objective analysis methodology may also help to improve the accuracy of mapped fields (Zhou, 1998; Lynch and McGillicuddy, 2001).

c. Simulation model

Circulation on Georges Bank and the adjacent waters results from a complex combination of processes driven by a variety of different forcing mechanisms. The conceptual model that has emerged from a number of different investigations (Butman *et al.,* 1987; Naimie *et al.,* 1994; Beardsley *et al.,* 1997) is composed of five different circulation elements: (1) rectification of strong tidal currents which creates a clockwise circulation around the Bank; (2) seasonal stratification and associated tidally induced frontal structures which tend to reinforce the tidally rectified circulation; (3) wind stress variations which at times can cause significant cross-isobath flow; (4) a shelf-slope front that dominates the flow seaward of the 100 m isobath along the Southern Flank; and (5) an externally imposed along-shelf pressure gradient.

A numerical model that includes representations of all these processes has been developed at the Dartmouth Numerical Methods Laboratory (Lynch *et al.,* 1996). A finite element approach has been utilized, facilitating realistic representation of the complex geometry in this area. Horizontal grid spacing in regions of steep topography is as fine as 500 m and considerably coarser where such high resolution is not required. The three-dimensional model is hydrostatic, nonlinear, and incorporates advanced turbulence closure. Published solutions for the climatological mean eulerian circulation, broken down into six bi-monthly periods, are demonstrably consistent with available observations (Naimie, 1996; Naimie *et al.,* 2001).

Archived solutions of the hydrodynamic model are stored in a form which is available for use in an off-line transport code "Acadia" which solves a depth-integrated form of the advection-diffusion-reaction equation on the same grid using the archived hydrodynamic information as input. Within this framework, the coupled physical-biological model for vertically averaged zooplankton concentration C is written

$$\frac{\partial C}{\partial t} + \mathbf{v} \cdot \nabla C - \frac{1}{H} \nabla \cdot (HK \nabla C) = R \tag{1}$$

where **v** is the velocity, K the diffusivity, H the bottom depth, and R the biological "reaction" term. Positive R implies a net biological source (e.g., growth), while negative R implies a net biological sink (e.g., mortality). Climatological mean velocity and diffusivity fields are specified from the bi-monthly archive described above. Boundary conditions consist of (1) no flux through solid boundaries, (2) specification of concentration at inflow, and (3) computation of concentration at outflow assuming no diffusive flux (i.e. $K\nabla C \cdot \hat{n} = 0$). No behavior is specified in the model, so the organisms are treated as passive tracers.

d. Data assimilation

The adjoint method of data assimilation facilitates inversion for the population dynamics implied by the changes in abundance between two successive surveys and the circulation during the intervening period. The approach begins with the definition of a cost function, which is a measure of the misfit between predicted and observed concentrations. The goal of the procedure is to minimize the cost function, subject to the constraint that the forward model equation is obeyed. Formulation of a Lagrange function, which is the sum of the cost function and the product of a set of Lagrange multipliers with the model equations, facilitates derivation of the adjoint model. Its exact form depends on the nature of the biological reaction term and the chosen cost function. In this study, the biological reaction term $R = R(x, y)$ is a spatially varying constant that does not change in time during the interval over which the data are being assimilated[4] (four separate one-month periods are used here). Defining the cost function as the sum of squares of differences between predicted and observed concentrations, the adjoint of Eq. (1) is

$$-\frac{\partial \lambda}{\partial t} - \nabla \cdot (\lambda \mathbf{v}) - \frac{1}{H}\nabla \cdot (HK\nabla\lambda) = -2\delta_M(C - C_{obs}) \tag{2}$$

where λ are the Lagrange multipliers and δ_M is a measurement functional which is equal to one where observations exist in space-time and zero elsewhere. Dynamically analogous to the forward model, the adjoint model is an advection-diffusion-reaction equation that describes the propagation of information about misfits between predicted and observed concentrations. It can be shown that integration of the adjoint equation provides a method of computing the gradient of the cost function with respect to the unknown variable $R(x, y)$.[5] This provides the basis for an iterative solution to the minimization problem that

4. Note that $R(x, y)$ therefore represents a temporal average of sources and sinks that occur during the month-long period between surveys. Clearly, many processes in the ocean occur on time scales shorter than one month. However, allowing for temporal variations in R would add even more degrees of freedom to a problem that is already underdetermined. Therefore we solve for $R(x, y)$, recognizing that it reflects the net result of processes that vary in time as well as space.

5. In this particular application, all of the model-data misfits are attributed to biological processes. Thus, the assimilation procedure will amalgamate any errors in the prescribed circulation into the inversion for $R(x, y)$. The implicit assumption here is that errors in the physics are small relative to biological sources and sinks.

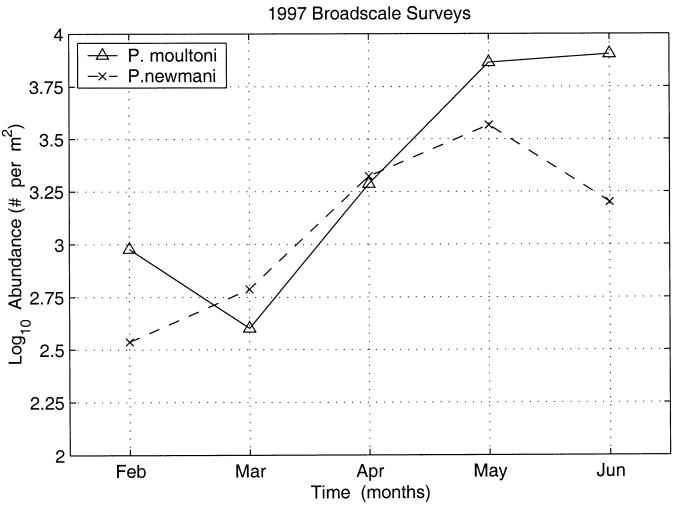

Figure 2. Seasonal variation in the vertically integrated (0–40 m) abundance of *P. moultoni* and *P. newmani* based on the 1997 broad-scale surveys. Monthly averages were computed with a simple arithmetic mean of the ensemble of stations from each survey (station positions are indicated in the top rows of Figs. 3 and 4).

consists of the following steps: (1) starting with some initial guess of the unknown variable (e.g., $R = 0$), initialize with data from the first survey and run forward in time to evaluate the cost function; (2) integrate the adjoint model, forced by the misfit between observed and predicted values to evaluate the gradient of the cost function with respect to the unknown variable; (3) feed the cost function and its gradient into a descent algorithm to yield an updated estimate of $R(x, y)$; and (4) repeat as necessary until convergence is attained. In practice, the assimilation procedure produces solutions for the concentration fields that are nearly identical to the objectively mapped observations. For more details on the method and its application to aggregate *Pseudocalanus* spp. populations in the Georges Bank/Gulf of Maine region, see McGillicuddy *et al.* (1998). Also see Matear and Holloway (1995) in which a similar approach is used to investigate phosphorus cycling in the North Pacific.

3. Results

a. Descriptive analysis of the observed distributions

Spatial averages of the vertically-integrated abundance of the two species reveal significant month-to-month variability (Fig. 2). The abundances of both species increase dramatically during the spring growing season from March to May/June. This pattern is consistent with what has been reported previously for the genus *Pseudocalanus* on Georges Bank (Davis, 1987). Despite the similarity in monthly variations of mean abundances, the spatial distributions of *P. moultoni* and *P. newmani* are quite distinct (Figs. 3 and 4, top

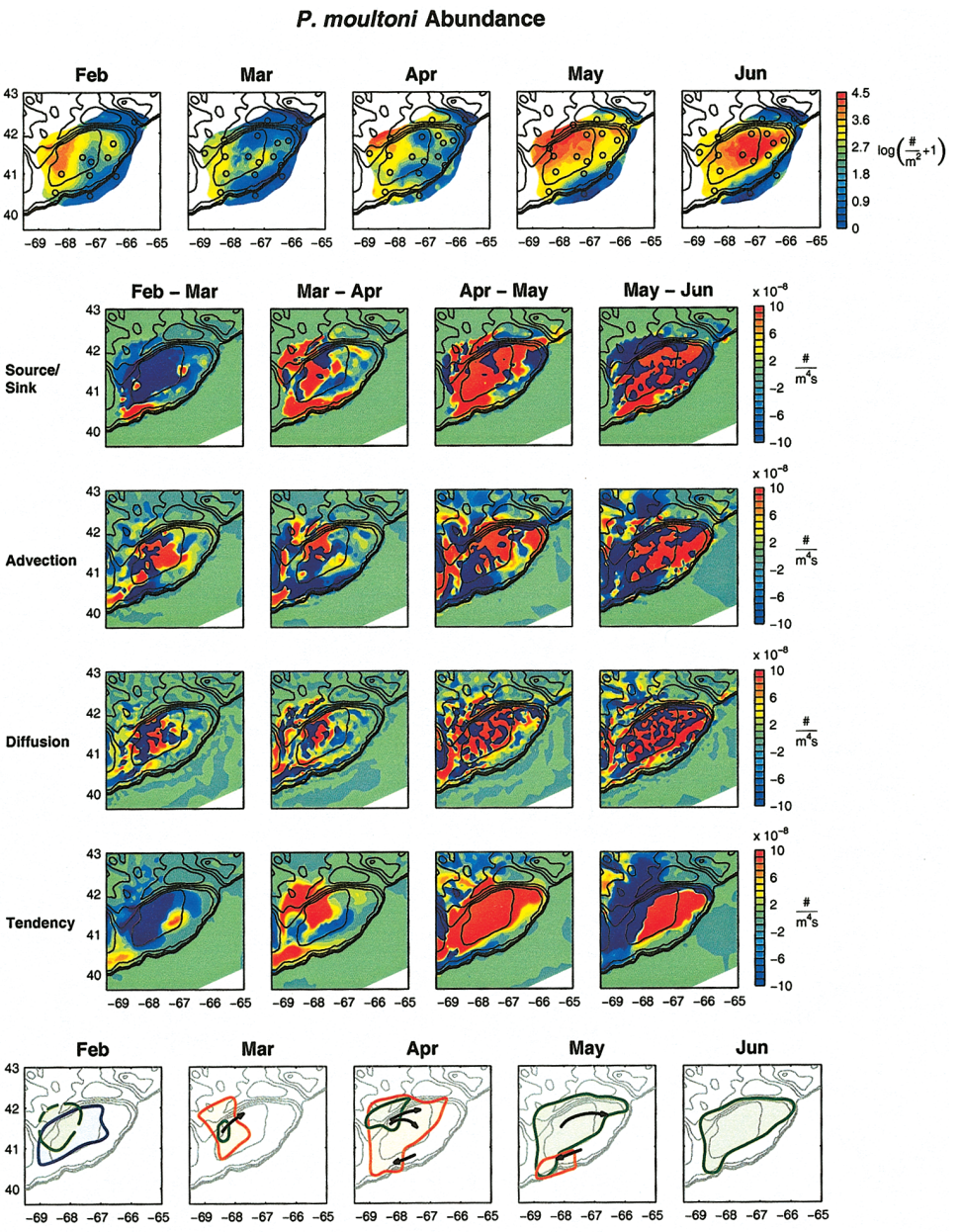
P. moultoni Abundance
Feb
Mar
Apr
May
Jun
43
42
41
40
−69 −68 −67 −66 −65
4.5
3.6
2.7
1.8
0.9
0
log(#/m²+1)
Feb – Mar
Mar – Apr
Apr – May
May – Jun
Source/ Sink
Advection
Diffusion
Tendency
x 10⁻⁸
10
6
2
−2
−6
−10
#/m⁴s

Figure 3.

rows). These patterns in vertically averaged abundance are similar to those in the two depth strata reported in Bucklin *et al.* (2001). Their general features are described below.

In February, prior to the onset of the growing season, the population centers of the two species appear to be co-located on the northwest portion of the Crest. However, the peak in *P. newmani* at this location is clearly an artifact of the objective analysis, as there are no observations within that feature. It appears that the peak is a result of extrapolation from the local minimum located just to the south on the Southern Flank. Thus the appropriate interpretation of the February map of *P. newmani* abundance is relatively low concentration in all areas sampled except for the southern tip of Browns Bank, where the concentration is moderately high. The peak in *P. moultoni* abundance on the northwest portion of the Crest also lacks observations to delimit it, although a contiguous high value is clearly present at the station in the southwest corner of the Crest.

Abundance of both species declines on Georges Bank in March. Bank-wide distributions vary inversely with each other: *P. moultoni* abundance is highest on the central portion of the Bank where *P. newmani* is nearly absent. High concentrations of *P. newmani* are found offshore of the shelf break on the Southern Flank; these patches are largely responsible for the slight increase in overall abundance of *P. newmani* in March. Moderately high concentrations persist on the southern tip of Browns Bank.

The growing season begins in April. *P. moultoni* abundance generally increases across the Bank, with particularly high concentrations on the northwest flank. In contrast, *P. newmani* is nearly absent from the Crest. High concentrations are present in a strip extending from the southern tip of Browns Bank across the Northeast Channel to the Northeast Peak and down along the Southern Flank between the 60 m and 100 m isobaths.

←

Figure 3. Top row: Monthly distributions of *P. moultoni* based on the U.S. GLOBEC Georges Bank broad-scale surveys for 1997. Vertically-integrated abundance (number of individuals per square meter) from net tows (stations indicated by open circles) were objectively analyzed onto a finite element mesh (see text). The geographic coverage of the maps is confined to that area where the expected error computed in the objective analysis, averaged over all time periods and both species, is less than approximately 70 percent. This error threshold was subjectively chosen to define a consistent mapping area that encompasses all of the broad-scale stations. Second row: Source terms $R(x, y)$ inferred from the adjoint data assimilation procedure. Each $R(x, y)$ is located directly below the two sets of observations used to drive the inversion. That is, initializing the forward model with the February observations and forcing it with the Feb–Mar source term will yield a simulation that matches the March observations. Third through fifth rows: the remaining terms in the ADR equation averaged over the period of integration: advective flux divergence, diffusive flux divergence, and overall tendency. Fields in the second through fifth rows have been normalized to the bottom depth, so the units are number of individuals per m^4 per second. The sign convention is such that the overall tendency equals the sum of advection, diffusion and source terms. Bottom row: schematic interpretation of the inversion results (see text). Green contours indicate population centers; biological sources and sinks are shown as red and blue contours, respectively. Advective impacts are denoted with black arrows. Ambiguous features of the schematics are dashed.

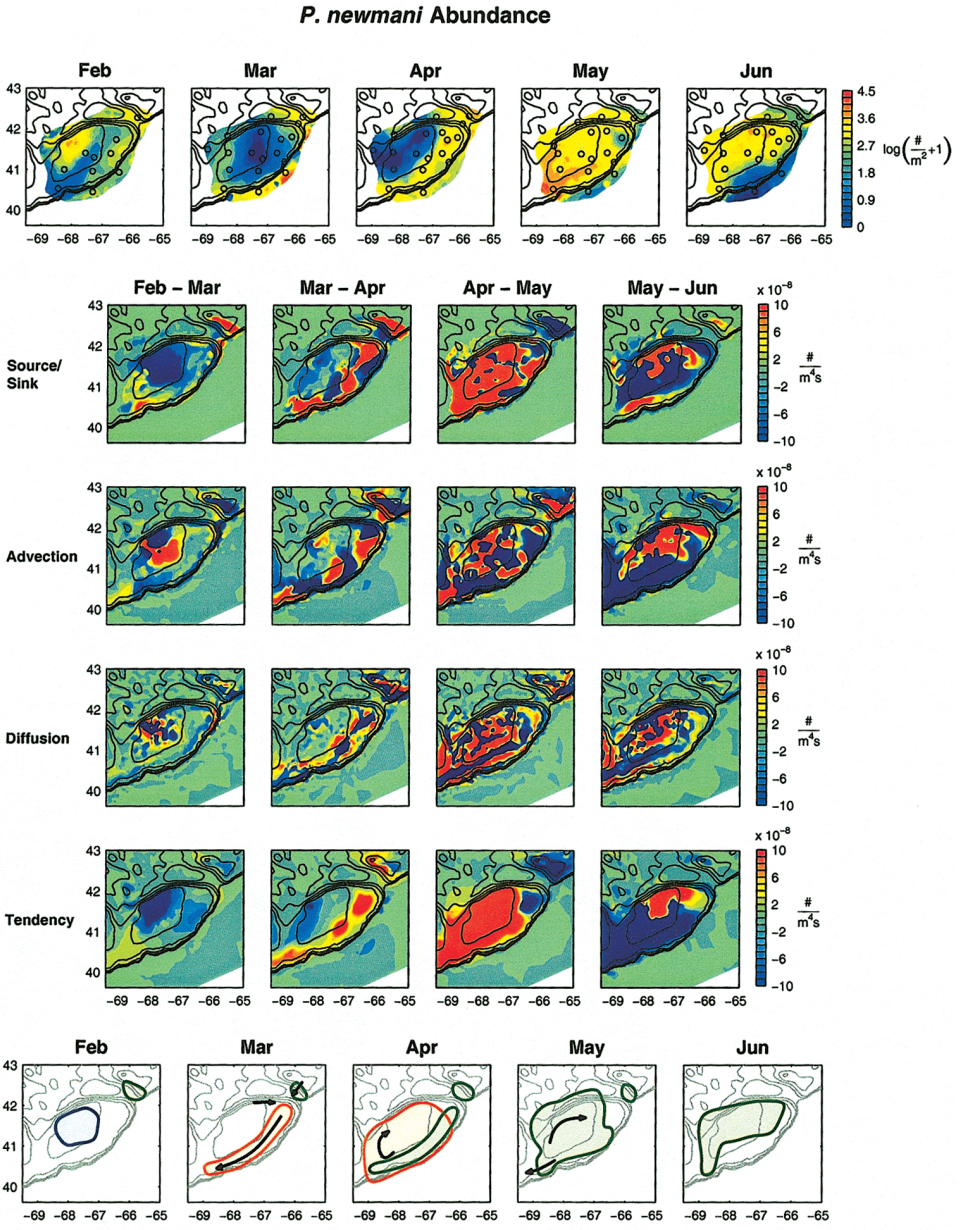

Figure 4. Same as Figure 3, but for *P. newmani.*

Both species continue their rapid increase in abundance in May. Very high concentrations of *P. moultoni* are present across the Bank, except for a southwest-to-northeast strip on the Southern Flank between the 68W and 66W meridians. Once again, *P. moultoni* is most abundant on the northwest flank of the Bank, resulting in an overall distribution with a centroid that is north and west of the center of the Bank. *P. newmani* occupies the Crest in significant numbers for the first time in May. Its highest abundance on the Bank continues to be located between the 60 m and 100 m isobaths on the Southern Flank, where *P. moultoni* is almost always in low abundance.

The springtime population increases of both species end by June. Overall abundance of *P. moultoni* changes very little from May to June, but its center of mass shifts eastward so that the area of highest abundance extends from the eastern portion of the Crest out to the Northeast Peak. *P. newmani* is similarly distributed, with moderately high concentrations along the northern half of the Bank. For the first time, abundance of *P. newmani* on Browns Bank is low. The area of low abundance on the Southern Flank in the June map is not well constrained by observations (due to missing stations in that area). This feature between the 60 m isobath and the shelf break is due to interpolation between high values on the Crest and low values in the deep waters off the Southern Flank. Based on the available data, it is not possible to quantify the abundance of either species on the Southern Flank in June.

b. Convergence of the inverse solutions

Satisfactory convergence of the solutions was obtained, as evidenced by the substantial reduction of model-data misfits in all cases (Fig. 5). The inversion procedure is relatively efficient, in that most of the improvement in the cost function occurs within the first ten iterations. The final value of the cost function depends on the specifics of each case: the animal distributions, the hydrodynamic fields, and their mutual orientation. In most instances, the fit to observations is improved by an order of magnitude in comparison to the solution forced by the "first guess" of $R(x, y) = 0$ (i.e. no biological sources or sinks). In general, the forward model predictions based on the final estimate (the 50th iteration) of $R(x, y)$ are nearly indistinguishable from the observations.

c. Uniqueness of the inverse solutions

Although it is not possible to demonstrate *a priori* that the assimilation procedure results in a global minimum of the Lagrange function, the existence of local minima can be investigated by starting from different initial guesses of the control variables. A suite of additional experiments was conducted using different random distributions to initialize R, and each case converged on the same solution. This, together with the fact that the resulting forward model predictions are nearly identical to the data, attests to satisfactory solution of the minimization problem.

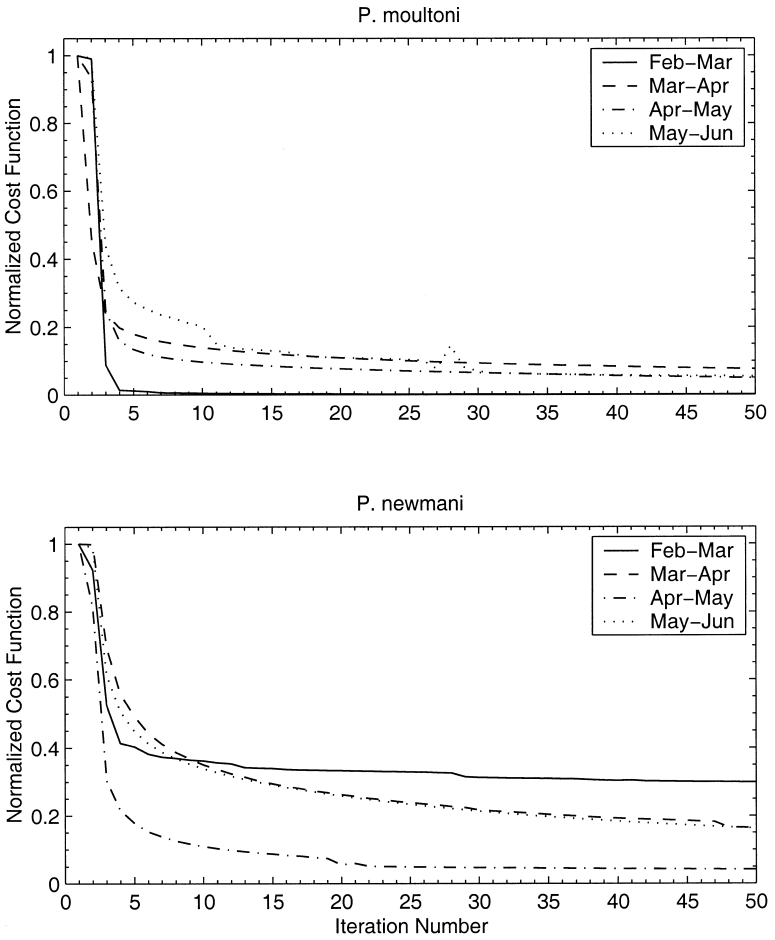

Figure 5. Convergence of the inverse solutions for *P. moultoni* (top) and *P. newmani* (bottom). The cost function J is defined which is a measure of the misfit between predicted and observed concentrations C_{obs}: $J = \int_0^{L_x} \int_0^{L_y} \int_{t_0}^{t_1} \delta_M (C - C_{obs})^2 dx dy dt$, where L_x and L_y define the extent of the model domain, and δ_M is a measurement functional which is equal to one where observations exist in space-time and zero elsewhere. For clarity in presentation, each of the curves above has been normalized to the initial value of J (i.e. the cost function for a forward model run with $R = 0$).

d. Description of the inverse solutions

The biological sources and sinks of the two species implied by the observed changes in abundance and the underlying circulation are quite distinct (Figs. 3 and 4). Using this information together with maps of the remaining terms in the advection-diffusion-reaction equation, the dynamical balances controlling the observed variations can be diagnosed. Generally speaking, the sources and sinks counterbalance the effects of advection to

produce the observed temporal changes. Although the magnitude of the diffusive flux divergence is often comparable to the other terms, diffusion tends to operate on much smaller spatial scales and is therefore mostly responsible for smoothing out peaks in the simulated distributions. The detailed evolution of the monthly term balances is summarized below for both species. In this discussion, biological sources and sinks are referred to as "growth" and "mortality," respectively.

i. February to March. The decline in abundances of both species on Georges Bank is for the most part due to an area of high mortality centered on the crest of the Bank. Organized structure is present in the advective flux divergence, where transport of the organisms by the mean current results in (1) removal in areas where the peak abundances were present in February, and (2) supply in adjacent areas located slightly downstream. Advective dilution (i.e. delivery of low-concentration water) tends to reinforce net mortality on the northern and western portions of the Crest. Although the advective source counterbalances to some degree the mortality on the southern and western flanks of the Crest, the net biological sink generally overshadows the advective contribution. However, it should be noted that the strongest advective signals are associated with peaks in the distributions of both *P. moultoni* and *P. newmani* on the northwest portion of the Crest that are not constrained by observations. As described above, these features are artifacts of the objective analysis. Therefore, these advective dynamics are not reflected in the schematic summary shown in the bottom rows of Figures 3 and 4.

ii. March to April. The observed increase in *P. moultoni* on the northwest portion of the Bank in April is driven by a combination of advection and a local biological source. The maximum in the population located on the western side of the Crest in March is transported in the clockwise around-bank flow, during which it is augmented by local reproduction. In addition, strong biological sources arise in the deep waters northwest of the Bank, resulting in the large increase in abundance observed on the Bank's northwest margin in April. Based on this analysis it is not possible to determine whether or not this is a result of local reproduction for the following reason. In the absence of any data upstream, the concentration in the incoming waters is assumed to be zero. This causes the advective contribution to the term balance to be negative, due to the dilutive influence of upstream waters. The inversion procedure is, therefore, forced to create the increase in abundance in this area via a local source.

In contrast, the most striking changes in the *P. newmani* distribution during this time period occur on the Southern Flank. The dramatic increase in abundance on the Southern Flank is driven by a biological source that extends from the Northeast Peak all the way down the Southern Flank. The details of the distribution are modified by smaller-scale patches of net mortality. The issue of linkage between the population centers on Browns Bank and the Northeast Peak is complex. The biological sources and sinks on the southwest portion of Browns Bank essentially mirror the advective flux divergence. There

is a very clear advective source in the Northeast Channel, suggesting transport of the Browns Bank population toward the Northeast Peak. However, the primary source waters for the Northeast Peak represented in the climatology during this time period lie to the west, where *P. newmani* concentrations are very low—thereby causing advective dilution centered on the Northeast Peak. The degree to which Browns Bank seeds the Georges Bank population of *P. newmani* depends critically on the relative contributions of sources from the Scotian Shelf and Northern Flank in forming the mixture of water occupying the Northeast Peak. We will return to this issue in the Discussion.

iii. April to May. A large area of net growth leads to expansion of the *P. moultoni* population center from the northwest corner of the Bank in April to cover most of the northern two-thirds of the Bank in May. Advection helps to fill in the eastern portion of the Bank as high concentrations from the western side of the Crest are transported in the around-bank flow. Note that the region of negative advective flux divergence extends southward all the way to the shelf edge. The southern portion of this advective sink results from low-concentration water flowing southwestward along the Southern Flank. The relatively high abundance observed on the southwest corner of the Bank in May implies a biological source in that area, which could be accounted for by local reproduction. Alternatively, the high abundance on the southwest corner could result from southward transport of high-concentration water from the northwest corner down through the Great South Channel. Unfortunately the data do not extend far enough west to assess the latter possibility.

A nearly bank-wide biological source is required to account for the dramatic increase in *P. newmani* from April to May. Unlike every other case examined herein, it is difficult to identify a systematic impact of advection during this period in which the *P. newmani* population dynamics are so dominated by reproduction. The advective flux divergence takes on a mottled form with a myriad of small-scale features. Perhaps the only coherent structure in the field is made up of the mostly positive contributions on the western side of the Crest. This advective source is associated with penetration of high-concentration water from the Southern Flank as it turns northward toward the Crest.

iv. May to June. The eastward shift of the *P. moultoni* distribution from May to June is caused by a mixture of advection and biological sources and sinks. Although there are many fine-scale details, the main signal in the advective flux divergence on the northernmost two-thirds of the Bank is removal from the western side and delivery to the eastern side. Smaller-scale features in the biological source term serve to modify the detailed structure of the distribution, but advection tends to dominate during this time period in which the overall abundance of *P. moultoni* is relatively stable. Note that high concentrations persist on the southwest corner of the Bank. As in the prior period, this implies a biological source slightly upstream on the Southern Flank.

The overall decline in abundance of *P. newmani* from May to June is in large measure a result of advective loss from the western portion of the Southern Flank. With the removal

of this concentration maximum from the southwest corner, the center of mass of the population shifts to the northern half of the Bank, with a maximum located where the 60 m isobath turns southward. This feature of the distribution is heavily influenced by advective supply from the southern and western portions of the Crest, delivered by the around-bank flow. Small-scale features in the biological source term on the northern half of the Bank modify the details of the distribution. Note the gap in observations between the 60 m and 100 m isobaths on the Southern Flank in June; clearly the dynamics of the coupled model are not well constrained in that region.

4. Discussion

a. Interpretation of the reaction term

It is of considerable importance to determine whether or not the biological rates inferred in this study are consistent with what has been measured in the laboratory and in the field. The magnitude of the reaction term varies from about -100 to $+100$ individuals m^{-3} day^{-1}, with almost all of the values falling between -10 and $+10$. Note that these are absolute rates of population change, not specific rates. Furthermore, these values represent the net effect of all biological sources (e.g., C5 copepodites molting to adults) and sinks (e.g., consumption by predators). Thus, it is to be expected that the distribution of inferred values $R(x, y)$ should be bounded by measurements of the population dynamics processes themselves.

This is, in fact, the case. For example, the rate of molting from C5 copepodites to adults can be estimated from the observed abundance of C5s and knowledge of their food-satiated, temperature-dependent development times. This computation can be justified on the basis of laboratory rearing experiments (Davis, 1984c) that demonstrate *Pseudocalanus* spp. development is not limited by food availability at chlorophyll concentrations present on Georges Bank. According to data from 15–30 liter pumped samples filtered through a 40-micron mesh, the mean abundance of C5 copepodite *Pseudocalanus* spp. was approximately 1000 individuals m^{-3} in April 1997, 6000 individuals m^{-3} in May 1997, and 1000 individuals m^{-3} in June of 1995 (data courtesy of Dr. Lewis Incze, available in the U.S. GLOBEC database http://globec.whoi.edu). Using a characteristic C5 abundance of 2500 individuals m^{-3} and a typical duration in that stage of 5 days at ambient temperatures on Georges Bank (McLaren *et al.,* 1989) results in a flux of C5 to adults on the order of 500 individuals m^{-3} day^{-1}. None of the inferred reaction rates in the inverse solutions exceed this value.

A lower bound for the reaction term can be estimated from information on mortality. *Pseudocalanus* spp. is subject to predation from a variety of other animals, including chaetognaths, ctenophores, and omnivorous copepods (e.g., Davis, 1984b; Sullivan and Meise, 1996; Sell *et al.,* 2001). In addition, voracious planktonic hydroids have recently been shown to exert significant predatory control on zooplankton populations (Madin *et al.,* 1996; Bollens *et al.,* 2001). Feeding experiments based on *Calanus finmarchicus*

nauplii suggest ingestion rates of approximately 0.25 copepods hydranth^{-1} day^{-1} at typical densities of copepods (Madin *et al.,* 1996). Although concentrations of hydroids as high as 25,000 hydranths m^{-3} have been observed, values of 10,000 are not uncommon. This indicates a potential consumption rate of 2,500 copepods m^{-3} day^{-1}. What would be the impact on adult *Pseudocalanus* populations simulated herein? *Pseudocalanus* represents approximately half of the total number of copepods (0.165 mm and larger) present on Georges Bank during the February to June time period (computed from information provided in Davis, 1987). Based on pump samples described above, adults comprise approximately 15% of the total post-larval population. Thus, hydroid predation on adult *Pseudocalanus* could be on the order of 200 individuals m^{-3} day^{-1} in areas where hydroids are present in average densities of 10,000 m^{-3}. Interestingly, hydroids appear to be most abundant in the shallower waters of the central Bank, where much of the net mortality inferred in this study occurs. This observational estimate of mortality of 200 individuals m^{-3} day^{-1} far exceeds the largest net sinks produced by the inverse technique. This is particularly striking given the fact that hydroids constitute only one component of the suite of predators that feed on *Pseudocalanus.*

Thus it is clear that the distribution of biological sources and sinks inferred with the adjoint method falls within the range of measured rates for processes intrinsic to the animals' population dynamics. Yet another potential source term arises from the joint effects of fluid motions and organism behavior. For example, upward-swimming animals will tend to accumulate in areas of surface convergence. Because behavior is not included in the present model, such effects are not represented explicitly in the solutions. Nevertheless, this coupled physical-biological process of aggregation may play a significant role in controlling plankton distributions on Georges Bank (e.g., Epstein and Beardsley, 2001) and therefore would be implicit in R. Future work will address this issue directly through inclusion of behavior in the model.

b. A conceptual model

Results of the inversions facilitate distillation of a conceptual model for how the distributions of the two species of *Pseudocalanus* evolve on Georges Bank (Fig. 6). In April, at the beginning of the growing season, the population centers of the two species are quite distinct: *P. moultoni* is located primarily along the northwest flank of the Bank, whereas *P. newmani* predominates on the Southern Flank and the southern tip of Browns Bank. The joint effects of advection and net growth of both species result in distributions that overlap in June. During the growing season, the around-bank flow amalgamates the two reproducing (but not interbreeding) populations such that their initially separate centers of mass become coincident. In essence, the circulation (i.e. the combined effects of advection and diffusion) mixes the two species from their respective source regions into an overall distribution that is centered on the Bank by the end of the growing season.

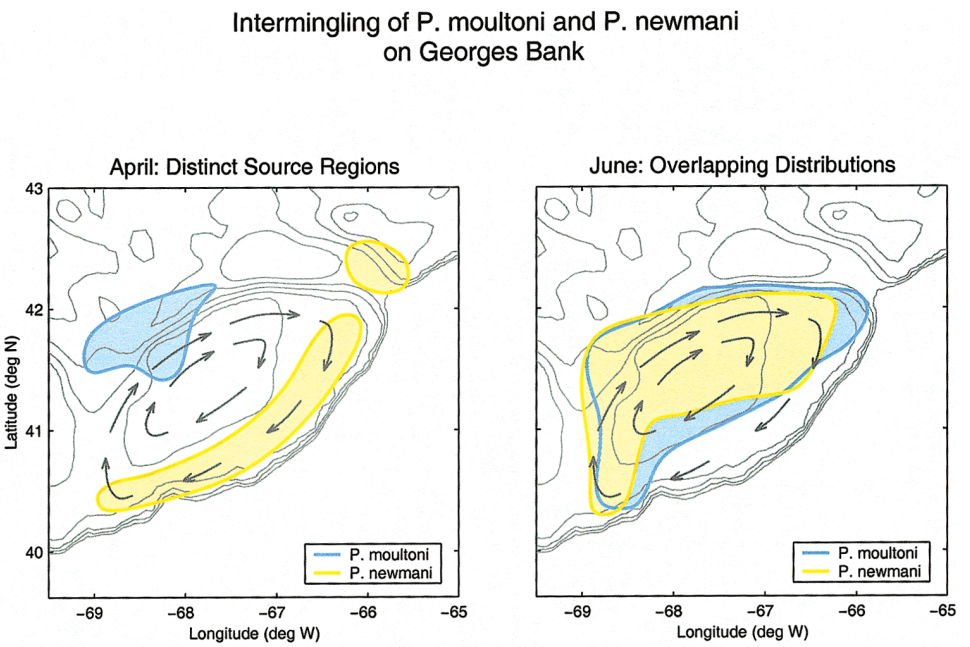

Figure 6. Intermingling of *P. moultoni* and *P. newmani* during the growing season on Georges Bank. Contours outlining the population centers of the two species for April and June are the same as in the schematics in the bottom rows of Figures 3 and 4. The clockwise circulation on Georges Bank is depicted by arrows.

c. Caveats

There are a number of caveats that must be considered in the interpretation of this conceptual model. To begin with, this analysis is based on species counts in stratified samples from the upper 40 m of the water column. Although species-level enumeration of *Pseudocalanus* spp. from deeper strata is not available, comparison of total counts above and below 40 m indicate that approximately 45% of the population is below this level. However, independent analysis of samples from two strata (0–15 m and 15–40 m), indicates that spatial patterns are generally coherent in the upper water column. Thus, it seems unlikely that inclusion of the deeper animals would materially alter the conceptual model unless they were all of only one species.

It is also important to recognize limitations of the assimilation procedure used herein. First of all, the physical transport fields are assumed to be perfect. If changes in abundance are incompatible with the prescribed circulation, the inversion technique will construct the $R(x, y)$ necessary to make up for that discrepancy. In this sense, it is possible for deficiencies in the circulation model to lead to anomalous biological sources and sinks. Alternatively, $R(x, y)$ can be interpreted as the sum of biological processes plus the net impact of any departures from the prescribed circulation. However, the most salient

characteristics of the solutions presented here are associated with robust features of the circulation on Georges Bank that are well documented in the literature (Naimie, 1996; Naimie *et al.,* 2002). This is not to say that the vertically integrated transport model used here is completely sufficient, especially in stratified conditions. Furthermore, the potential for nonlinear impacts of time-dependent flows (such as storm events) on the mean behavior of the system remains to be investigated. Recent advances in physical oceanographic data assimilation methodology (Lynch *et al.,* 1998, 2001; Lynch and Hannah, 2001; Lynch and Naimie, 2001) will permit future studies of this type to be based on actual hindcasts of the circulation rather than climatology. In this context, it will be possible to investigate the sensitivity of the results to the details of the hydrodynamic fields by performing biological inversions on ensembles of circulation hindcasts that are all equally valid with respect to observations.

5. Conclusions

Species-level data have revealed rich structure in populations of *Pseudocalanus* in the Georges Bank/Gulf of Maine region. Observations from February to June of 1997 demonstrate that distributions of *P. moultoni* and *P. newmani* are distinct and vary seasonally. Assimilation of these data into a coupled physical-biological model facilitates investigation of the temporal linkage between monthly surveys. Inverse solutions indicate that *in situ* population dynamics and advective transport constitute roughly equal contributions to the observed temporal changes. The magnitudes of the inferred biological sources and sinks are not inconsistent with available rate measurements of population dynamics processes such as reproduction and mortality.

The seasonal progression of the adult distributions is as follows. Early in the growing season, the source of *P. moultoni* appears to be on the northwest flank of Georges Bank; for *P. newmani* it appears to be the Northeast Peak and the southern tip of Browns Bank. As the growing season progresses, the clockwise flow and lateral dispersion on Georges Bank blends the distributions of the two species such that they overlap by June.

This analysis provides some clues as to the likelihood that either of the two species might be self-sustaining on Georges Bank. The fact that there is an advective pathway returning adults to the source region suggests the *P. moultoni* is potentially an endemic species. Such is not necessarily the case for *P. newmani,* depending on the specifics of the source region: whether it is the Northeast Peak, Browns Bank, or both. The clockwise flow on Georges Bank clearly resupplies the Northeast Peak. However, there is no advective mechanism in the seasonally time-averaged flow for transport back to Browns Bank. If the ultimate source of these animals is in fact Browns Bank, then *P. newmani* is perhaps a transient resident on Georges Bank, destined for a transport pathway that prevents return to the source region. Water from the Scotian Shelf does in fact impinge on Georges Bank in intermittent "crossover" events across the Northeast Channel (e.g., Smith *et al.,* 2001). Thus it is not clear whether or not the portion of the "source" population of *P. newmani* observed on the Northeast Peak in April of 1997 was actually delivered from the Scotian

Shelf. Resolution of the source region for *P. newmani* will require further quantification of the linkage between Browns and Georges Banks. This has fundamental implications for the present conceptual model with respect to whether or not *P. newmani* can be self-sustaining on Georges Bank.

Of course, caution must be exercised in generalizing the interpretation of these results beyond the space and time scales explicitly resolved in this analysis. The monthly surveys utilized herein capture the springtime evolution of both species during the 1997 growing season. However, the question of whether or not either species is endemic begs for additional observations during the remaining portion of the annual cycle. Moreover, given the considerable interannual variability characteristic of this region, it is likely that several years worth of data will have to be synthesized in order to distill a robust conceptual model of the oceanographic ecology of the genus *Pseudocalanus* in this region. This study demonstrates that a species-level approach will be required in order to do so.

It is also worth noting a rather general feature of the inverse solutions reported here and in other studies utilizing similar methodology on different zooplankton data sets in this region (McGillicuddy *et al.,* 1998; 2001). That is, the inferred biological sources and sinks contain heterogeneity on spatial scales comparable to (and in some cases smaller than) the patchiness of the observed abundance patterns. This result is somewhat troubling because practical considerations preclude obtaining observational rate estimates with the same space/time resolution at which abundance is measured. Independent verification of the inverse solutions therefore must rely on rather coarse comparisons. For example, in the present study it was shown that the inferred biological sources and sinks are bounded by experimentally-determined rates of population growth and predation. In future work, we intend to incorporate explicit population dynamics into the forward model, including temperature and food-dependent development as well as mortality based on measured abundances of dominant predators. In addition, use of a bulk-sample assay for species identification of pre-adult stages of *Pseudocalanus* will provide valuable additional constraints on processes controlling the adult distributions. Taken together, more sophisticated models and stage-based observations may help explain some of the "mesoscale" structure in biological processes suggested by the simple inversions described herein. More generally, the union of such models with observations in the context of formal mathematical inversion will provide a framework for testing our understanding of the mechanisms controlling planktonic populations in the ocean.

Acknowledgments. We gratefully acknowledge the support of NSF and NOAA in this effort. We thank Valery Kosnyrev for objective analysis of the observations, as well as technical assistance in interpreting the results. Olga Kosnyreva's skillful visualization of model outputs in both animated and image format is greatly appreciated. We thank Lew Incze for his observations of *Pseudocalanus* larval abundances which helped constrain estimates of various population dynamics rates. We thank Professor Edward Durbin and two anonymous reviewers for valuable comments that helped improve the manuscript.

This is WHOI contribution 10599 and U.S. GLOBEC contribution 342.

REFERENCES

Beardsley, R. C., B. Butman, W. R. Geyer and P. Smith. 1997. Physical oceanography of the Gulf of Maine: an update, *in* Proceedings of the Gulf of Maine Ecosystem Dynamics Scientific Symposium and Workshop, Regional Association for Research in the Gulf of Maine, Hanover, NH, RARGOM Report 97-1, 39–52.

Bollens, S. M., E. Horgan, S. Concelman, L. P. Madin, S. M. Gallager and M. Butler. 2001. Planktonic hydroids on Georges Bank: effects of mixing and food supply on feeding and growth. Deep-Sea Res. II., *48,* 659–672.

Bretherton, F. P., R. E. Davis and C. B. Fandry. 1976. A technique for objective analysis and design of oceanographic experiments applied to MODE-73. Deep-Sea Res., *23,* 559–582.

Bucklin, A. 2000. Methods for population genetic analysis of zooplankton, *in* The Zooplankton Methodology Manual. International Council for the Exploration of the Sea, Academic Press, London, 533–570.

Bucklin, A., A. M. Bentley and S. P. Franzen. 1998. Distribution and relative abundance of the copepods *Pseudocalanus moultoni* and *P. newmani* on Georges Bank based on molecular identification of sibling species. Mar. Biol., *132,* 97–106.

Bucklin, A., M. Guarnieri, D. J. McGillicuddy and R. S. Hill. 2001. Spring-summer evolution of *Pseudocalanus* spp. abundance of Georges Bank based on molecular discrimination of *P. moultoni* and *P. newmani.* Deep-Sea Res. II., *48,* 589–608.

Bucklin, A., R. S. Hill and M. Guarnieri. 1999. Taxonomic and systematic assessment of planktonic copepods using mitochondrial COI sequence variation and competitive, species-specific PCR. Hydrobiol., *401,* 239–254.

Butman, B., J. W. Loder and R. C. Beardsley. 1987. The seasonal mean circulation: observation and theory, *in* Georges Bank, R. Backus and D. Bourne, eds., MIT Press, Cambridge, 121–138.

Cohen, R. E. and R. G. Lough. 1982. Zooplankton distribution and abundance in the Georges Bank–Nantucket Shoals area during the autumn-winter larval Atlantic herring surveys (1973–1977). Technical Report 82-12, National Marine Fisheries Service, Woods Hole, MA.

Corkett, C. J. and I. A. McLaren. 1978. The biology of *Pseudocalanus.* Adv. Mar. Biol., *15,* 1–231.

Davis, C. S. 1984a. Interaction of a copepod population with the mean circulation on Georges Bank. J. Mar. Res., *42,* 573–590.

—— 1984b. Predatory control of copepod seasonal cycles on Georges Bank. Mar. Biol., *82,* 31–40.

—— 1984c. Food concentrations on Georges Bank: Non-limiting effect on development and survival of laboratory reared *Pseudocalanus* sp. and *Paracalanus parvus* (Copepoda: Calanoida). Mar. Biol., *82,* 41–46.

—— 1987. Zooplankton life cycles, *in* Georges Bank, R. Backus and D. Bourne, eds., MIT Press, Cambridge, MA, 255–268.

Epstein, A. W. and R. C. Beardsley. 2001. Flow-induced aggregation of plankton at a front: a 2-d eulerian model study. Deep-Sea Res. II, *48,* 395–418.

Foote, K. G. and G. Stefánsson. 1993. Definition of the problem of estimating fish abundance over an area from acoustic line-transect measurements of density. ICES J. Mar. Sci., *50,* 369–381.

Freeland, H. J. and W. J. Gould. 1976. Objective analysis of meso-scale ocean circulation features. Deep-Sea Res., *23,* 915–923.

Frost, B. W. 1989. A taxonomy of the marine calanoid copepod genus *Pseudocalanus.* Can. J. Zool., *67,* 525–551.

He, I., R. Hendry and G. Boudreau. 1997. OAX demonstration and test case. http://www.tuns.ca/~hey/ocean/oview.html.

Laurence, G. C. 1974. Growth and survival of haddock (*Melanogrammus aeglefinus*) larvae in relation to planktonic prey concentration. J. Fish. Res. Bd. Can., *31,* 1415–1419.

Lynch, D. R. and C. G. Hannah. 2001. Inverse model for limited-area hindcasts on the continental shelf. J. Atmos. Ocean. Technol., *18,* 962–981.

Lynch, D. R., J. T. C. Ip, C. E. Naimie and F. E. Werner. 1996. Comprehensive coastal circulation model with application to the Gulf of Maine. Cont. Shelf Res., *16,* 875–906.

Lynch, D. R. and D. J. McGillicuddy. 2001. Objective analysis for coastal regimes. Cont. Shelf Res., *21,* 1299–1315.

Lynch, D. R. and C. E. Naimie. 2002. Hindcasting the Georges Bank circulation, part II: Wind-band Inversion. Cont. Shelf Res., *22,* 2191–2224.

Lynch, D. R., C. E. Naimie and C. G. Hannah. 1998. Hindcasting Georges Bank circulation, part I: detiding. Cont. Shelf Res., *18,* 607–639.

Lynch, D. R., C. E. Naimie, J. T. Ip, C. V. Lewis, F. E. Werner, R. Luettich, B. O. Blanton, J. Quinlan, D. J. McGillicuddy, J. R. Ledwell, J. Churchill, V. K. Kosnyrev, C. S. Davis, S. M. Gallager, C. J. Ashjian, R. G. Lough, J. Manning, C. N. Flagg, C. G. Hannah and R. C. Groman. 2001. Real-time data assimilative modeling on Georges Bank. Oceanogr., *14,* 65–77.

Madin, L. P., S. M. Bollens, E. F. Horgan, M. Butler, J. Runge, B. K. Sullivan, G. MacPhee, E. Durbin, A. G. Durbin, D. Van Kueren, S. Plourde, A. Bucklin and M. E. Clarke. 1996. Voracious planktonic hydroids: unexpected predatory impact on a coastal marine ecosystem. Deep-Sea Res. II., *43,* 1823–1829.

Matear, R. J. and G. Holloway. 1995. Modeling the inorganic phosphorus cycle of the North Pacific using an adjoint data assimilation model to assess the role of dissolved organic phosphorus. Global Biogeochem. Cycles, *9,* 101–119.

McGillicuddy, D. J., D. R. Lynch, A. M. Moore, W. C. Gentleman, C. S. Davis and C. J. Meise. 1998. An adjoint data assimilation approach to diagnosis of physical and biological controls on *Pseudocalanus* spp. in the Gulf of Maine—Georges Bank region. Fish. Oceanogr., *7,* 205–218.

McGillicuddy, D. J., D. R. Lynch, P. Wiebe, J. Runge, W. C. Gentleman and C. S. Davis. 2001. Evaluating the U.S. Globec Georges Bank broad-scale sampling pattern with Observational System Simulation Experiments. Deep-Sea Res. II., *48,* 483–499.

McLaren, I. A., J.-M. Sevigny and C. J. Corkett. 1989. Temperature-dependent development in *Pseudocalanus* species. Can. J. Zool., *67,* 559–564.

Naimie, C. E. 1996. Georges Bank residual circulation during weak and strong stratification periods: prognostic numerical model results. J. Geophys. Res., *101,* 6469–6486.

Naimie, C. E., R. Limeburner, C. G. Hannah and R. C. Beardsley. 2001. On the geographic and seasonal patterns of the near-surface circulation on Georges Bank—from real and simulated drifters. Deep-Sea Res. II., *48,* 501–518.

Naimie, C. E., J. W. Loder and D. R. Lynch. 1994. Seasonal variation of the 3-D residual circulation on Georges Bank. J. Geophys. Res., *99,* 15967–15989.

Petrie, B. and J. Dean-Moore. 1996. Temporal and spatial scales of temperature and salinity on the Scotian Shelf. Canadian Technical Report of Hydrography and Ocean Sciences 177, Bedford Institute of Oceanography, Dartmouth, Nova Scotia.

Romaine, S. J., D. L. Mackas and M. C. Macaulay. 2002. Comparison of euphausiid population size estimates obtained using replicated acoustic surveys of coastal inlets and block average vs. geostatistical spatial interpolation methods. Fisheries Oceanogr., *11,* 102–115.

Sell, A. F., D. van Keuren and L. P. Madin. 2001. Predation by omnivorous copepods on early developmental stages of *Calanus finmarchicus* and *Pseudocalanus* spp.. Limnol. Oceanogr., *46,* 953–959.

Smith, P. C., R. W. Houghton, R. G. Fairbanks and D. G. Mountain. 2001. Interannual variability of boundary fluxes and water mass properties in the Gulf of Maine and Georges Bank. Deep-Sea Res. II., *48,* 37–70.

Sullivan, B. K. and C. J. Meise. 1996. Invertebrate predators of zooplankton on Georges Bank: 1977–1987. Deep-Sea Res. II., *43,* 1503–1519.

Zhou, M. 1998. An objective interpolation method for spatiotemporal distribution of marine plankton. Mar. Ecol. Prog. Ser., *174,* 197–206.

Received: *8 January, 2002;* revised: *8 July, 2002.*